Robotics Research 9: Proceedings of the Ninth International Symposium of Robotics Research (ISRR'99)
October 9-12, 1999, Snowbird, Utah, USA

Advances in Underwater Robot Vehicles for Deep Ocean Exploration: Navigation, Control, and Survey Operations

Louis Whitcomb*, Dana Yoerger, Hanumant Singh, and Jonathan Howland †‡

Abstract

This paper reports recent advances and open problems in navigation, control, and survey methodologies for underwater robotic vehicles. First, the technical challenges of underwater navigation are discussed. Second, an acoustic navigation system combining bottom-lock doppler sonar and time-of-flight long-baseline (LBL) navigation techniques, recently reported by the Authors, is reviewed. The performance of this system is examined in the context of recent deep-submergence operations with the Jason underwater robot. Third, principal theoretical and practical obstacles to the task of acoustic and optical undersea survey operations are reviewed. These issues are illustrated with acoustic bathymetric and optical photomosaic surveys performed by the authors during two recent deployments in the Mediterranean Sea.

1 Introduction

Underwater robots can now perform high-resolution acoustic and optical surveys in the deep ocean that previously were considered impractical or infeasible. For example, [35] reports a 1997 survey in which Jason and ARGO II underwater vehicles were deployed to survey a 2 square kilometer shipwreck site in the Pacific. This survey resulted in a bathymetric map of the site, 135,774 electronic still images (each covering about 7mx10m), and hundreds of hours of conventional and high-definition video.

The technical obstacles to underwater missions, however, differ from those in land, air, and space missions in several fundamental respects: First, the the rapid attenuation of acoustic and electromagnetic radiation in seawater severely restricts the range (and field of view) of high resolution acoustic and optical sensors. In consequence, high-resolution underwater survey sensors must be submerged to the immediate vicinity of a survey site — in sharp contrast to airborne and space-based survey sensors systems. Moreover, radio navigation techniques commonly employed in air and space operations do not function undersea. Second, the high ambient pressure of the underwater environment poses formidable design challenges both for (inhabited) submarined and (uninhabited) robots. At present, only a few of the world's submarines are capable if diving beyond 1000 meters in depth. Only one present-day operational research submersible can dive to 6500 meters [13]; none can dive to the ocean's deepest depths of 11,000 meters. In contrast, numerous underwater robots operate to 6000 meters [2], and one is capable of 11,000 meters operation [14]. Finally, in the case of untethered vehicles, underwater missions are limited not only by on-board battery storage capacity, but also by the severely limited bandwidth and delay inherent in underwater acoustic communication.

The objective of this paper is to report recent advances and open problems in underwater robotics, and to distinguish these problems from those found in land, air, and space robot missions. The first objective is to demonstrate that precision underwater vehicle navigation remains the principal obstacle to improved vehicle control, and to report recent advances. The second objective is to demonstrate that precise navigation and control is just one of several obstacles to precise, quantitative, and repeatable underwater survey operations. We argue that precision surveys require fusion of data from variety of imaging sensors with differing ranges, resolutions, and physical principles, and report recent advances.

These research problems and advances are illustrated with data from deployments, performed by the authors, of the JASON, ARGO-II, and DSL-120 underwater vehicles of the National Deep Submergence Facility (NDSF) of the Woods Hole Oceanographic Institution (WHOI). The NDSF robot systems have accrued over 450 days of at-sea science operations since 1993 in the service of the U.S. oceanographic research community.

2 Navigation and Control

Few techniques exist for reliable three-dimensional position sensing for underwater vehicles. Table 1 summarizes the sensors most commonly used to measure a vehicle's six degree-of-freedom position. While depth, altitude, heading, and attitude are instrumented with high bandwidth internal ("on-board") sensors, the standard method for full ocean depth XYZ acoustic navigation is 12 kHz long baseline ("12 kHz LBL") acoustic navigation [11, 17]. 12 kHz LBL typically operates at up to 10 Km ranges with a range-dependent precision of +/-0.1 to 10 Meters and update rates periods as long as 20 seconds. The precision and update rate of LBL position fixes can vary over several orders of magnitude depending on the acoustic frequency,

*Whitcomb is with the Department of Mechanical Engineering, 123 Latrobe Hall, Johns Hopkins University, 3400 North Charles Street, Baltimore, Maryland, 21218 USA, email: llw@jhu.edu.

†Yoerger, Singh, and Howland are with the Deep Submergence Laboratory, Department of Applied Ocean Physics and Engineering, Woods Hole Oceanographic Institution, Woods Hole, MA, 02543, USA, email: dyoerger@whoi.edu, hsingh@whoi.edu, jhowland@whoi.edu

‡The Authors gratefully acknowledge the support of the U.S. Office of Naval Research for JASON field experiments under grant #N00014-95-J-1237 and through subcontract #1716 of grant #N00014-99-1-0109 to the Institute for Exploration, Mystic, CT., and the National Science Foundation for operational support of the Deep Submergence Operations Group (DSOG) under Grant #OCE-9627160.

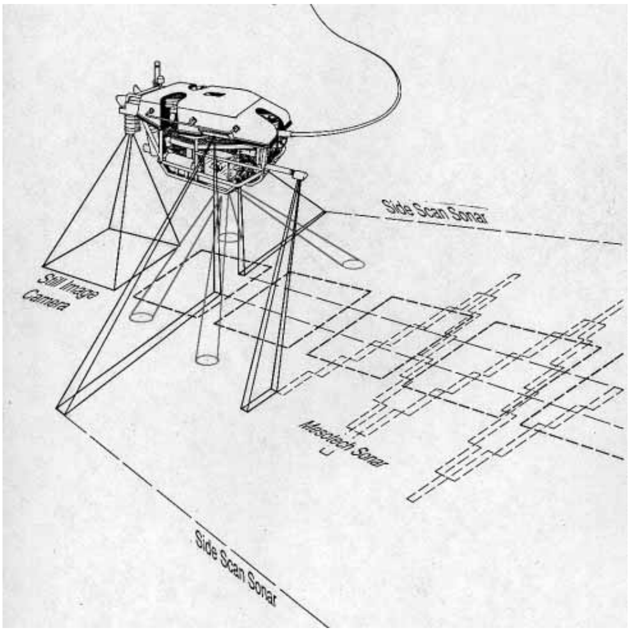

Figure 1: JASON, 6000 meter ROV, depicted in a survey operation showing electronic-still cameras, video cameras, scanning sonar, sidescan sonar, and doppler sonar beams. JASON was designed by the authors and collaborators, and is operated operated by the National Deep Submergence Facility of the Woods Hole Oceanographic Institution for use by the U.S. oceanographic research community.

range, and acoustic path geometry. LBL navigation accuracy and precision can be improved to some extent by careful application of Kalman or other filtering techniques [4, 30, 1].

An active area of active research in land, air, and undersea vehicles is "terrain relative" navigation — in which a vehicle uses real-time sensing and a terrain map (typically of topographic, magnetic, gravitational, or other geodetic data) to determine vehicle position. Authors have addressed the problem (*i*) where an *a-priori* map is available, e.g. [7, 18, 31]; (*ii*) the problem where *a-priori* maps are not available, but are constructed incrementally from sensor data, e.g. [19, 8]; and (*iii*) the problem where a task is achieved (e.g. altitude control, obstacle avoidance) without explicit maps, e.g. [38]. In typical underwater scientific missions, *a-priori* maps are seldom available. To the best of our knowledge, only approaches of type (*iii*) have been implemented and field-tested in real-time on operational underwater robot vehicles.

At present, the best method for obtaining subcentimeter XY position sensing is to employ a high-frequency (typically 300 kHz or greater) LBL system. Due to the rapid attenuation of higher frequency sound in water, high frequency LBL systems typically have a very limited maximum range. All transponder-based navigation methods require careful placement of the transponders, and are fundamentally limited by the speed of sound in water — about 1500 Meters/Second.

The precision of a 12 kHz LBL system is illustrated in Figure 2, showing JASON vehicle fixes obtained simultaneously using (a) 12 kHz LBL navigation and (b) 300 kHz LBL navigation. The data was obtained during survey operations during a Jason deployment in the Eastern Mediterranean Sea, dive #250, June 17, 1999, from 18:08Z to 19:34Z. The 12 kHz LBL update rate was 0.16 Hz (one fix every 6 seconds). The 300 kHz LBL update rate was 1.6 Hz (one fix every 0.6 seconds). The data show the 12 kHz LBL X and Y fixes to have zero mean and a standard deviation of 0.27 meter and 0.21 meter, respectively [33]. Note that these are unusually accurate LBL precision values — twice as accurate as reported for a previous deployment in [34].

The high LBL precision obtained in this 1999 deployment is the direct consequence of two factors: First, the shallow (500m) water depth and correspondingly short transponder ranges. Second, on this deployment we (for he first time) configured Jason's LBL system to perform a direct "Jason→Transponder→Jason" fix, rather than the more traditional "Ship→Transponder→Jason" or "Ship→Jason→Transponder→Ship" fixes. In consequence, the 1999 LBL errors are half that reported for previous deployments [34].

2.1 Doppler-Based Navigation

Recently available multi-beam doppler sonars can significantly augment the LBL navigation systems commonly employed for three-dimensional underwater robot vehicle navigation. A typical bottom-lock multi-beam sonar work as follows: The doppler transducer unit has four downward-looking beam transducers oriented at about 30° from the instrument vertical axis. A minimum of three beams are required; four are typically used. The resulting narrow beams are depicted in Figure 1.

First, the doppler sensor measures the apparent bottom-velocity (due to the vehicle's motion) along each of the four beams. The velocity measurement in broadband dopplers is performed with an ensemble of one or more discrete "pings" employing the entire set of four beams — this in contrast to some conventional doppler techniques that employ continuous tones. The doppler unit digitally processes the four ping responses to compute a 4×1 vector of velocities, $v_{beam}(t)$, representing the bottom velocity component along the respective beam axes. Single-ping velocity error standard-deviation varies with beam frequency. Velocity error standard-deviations vary with frequency and instrument design — our 1200 kHz unit provides a single-ping beam-velocity error standard deviation of 0.2%.

Second, the 4×1 vector of beam velocities, $v_{beam}(t)$, is converted to the instrument-frame XYZ velocities, $v_{instrument}(t)$, by a linear transformation

$$v_{instrument}(t) = T * v_{beam}(t). \tag{1}$$

The matrix T is a 4×4 constant matrix mapping the four beam velocities into a 4×1 vector of instrument velocities

$$v_{instrument}(t) = \begin{bmatrix} \dot{x}(t) \\ \dot{y}(t) \\ \dot{z}(t) \\ \dot{e}(t) \end{bmatrix} \tag{2}$$

representing the cartesian velocities $\dot{x}(t), \dot{y}(t)$, and $\dot{z}(t)$, in instrument-frame coordinates, and $\dot{e}(t)$, a least-square measure of the velocity error.

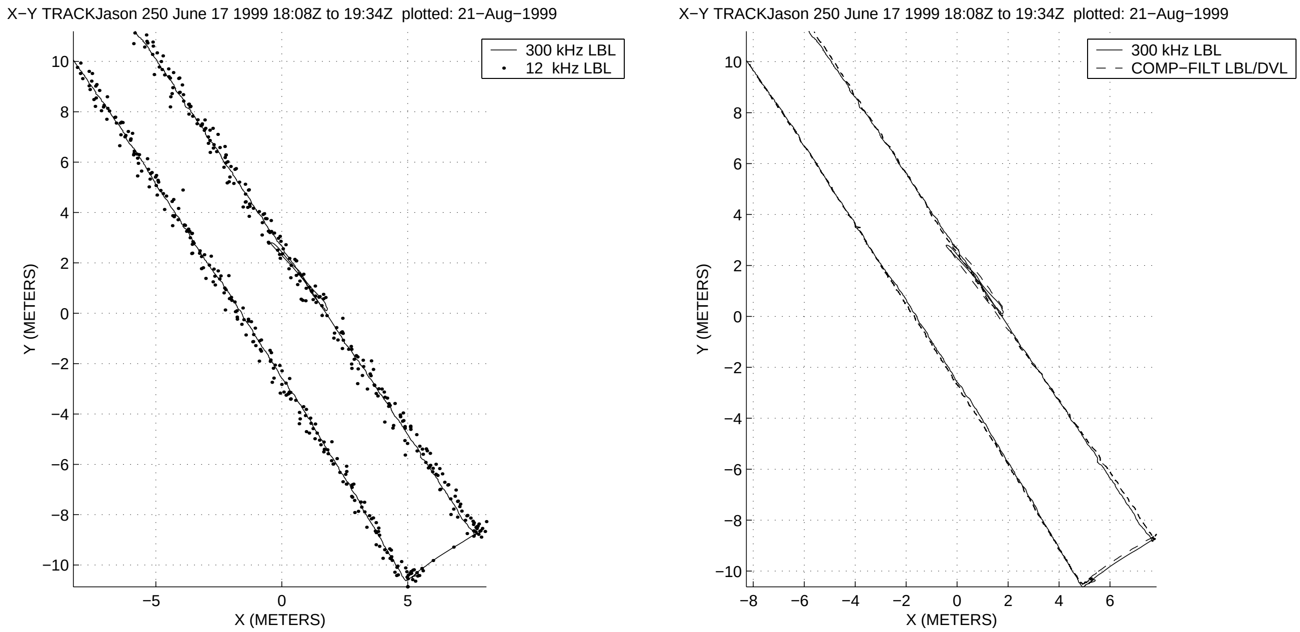

Figure 2: Navigation Precision: LBL (left) versus LBL/Doppler (right). Left graph shows X-Y Plot of 12 kHz LBL Jason position fixes (dots) and 300 kHz LBL X-Y fixes (solid line). Right graph shows X-Y Plot of LBL/Doppler Jason position fixes (dashed line) and 300 kHz LBL X-Y fixes (solid line). JASON dive #250 June 17 1999 18:08Z to 19:34Z.

Third, the 4×1 vector of instrument-frame velocities, $v_{instrument}(t)$, is converted to the world-frame XYZ velocities, $v_{world}(t)$, by the linear transformation

$$v_{world}(t) = \begin{bmatrix} R(t)_{3\times 3} & 0_{3\times 1} \\ 0_{1\times 3} & 1 \end{bmatrix} * v_{instrument}(t) \qquad (3)$$

where the orthogonal instrument-to-world rotation matrix, $R(t)$, is computed on-line from sensor values of roll, pitch, and heading.

Finally, the world velocities, $v_{world}(t)$, are integrated to compute bottom track position

$$x_{world}(t) = x(t_0) + \int_{t_0}^{t} v_{world}(\tau) d\tau \qquad (4)$$

where $x(t_0)$ is the user's initial position estimate. For a more detailed discussion of the doppler sensor equations and coordinate conversions, the reader is referred to [5, 23].

Previous Work

In [5, 6] Brokloff reports a bottom-lock doppler-based dead-reckoning system combining a 300kHz doppler and an inertial navigation unit (for vehicle heading and attitude data) to obtain relative navigation errors of 0.4% of distance traveled over long (five hour) high-speed (five knot) missions. In [26] Spindel reports an acoustic navigation system combining LBL navigation with continuous-tone doppler transponder beacons. In [34] the authors report preliminary results from the first deployment of the combined LBL/Doppler navigation system described herein. In [32] the authors identify principal limitations to the bottom-track precision of doppler based navigation systems and analyze the effect of heading-sensor errors on doppler bottom-track precision.

2.2 Combined Doppler/LBL Navigation

To take advantage of the incremental precision of the doppler with the absolute (but noisy) precision of the LBL, we have implemented a system utilizing complementary linear filters to combine low-passed LBL position fixes with high-passed doppler position fixes. The time constant of both filters was set to 120 Seconds. This system employed a conventional magnetic heading compass and conventional gravitational roll/pitch sensors. Note that in normal operation this system requires only standard LBL sea-floor transponders — in contrast to previously reported LBL+doppler systems which utilize additional fixed sea-floor mounted continuous-tone beacons [26].

For these experiments, JASON's standard suite of navigation sensors were augmented with new sensors listed in Table 1. JASON's experimental configuration is depicted in Figure 1. The experiments were conducted with the JASON ROV during an oceanographic deployment from aboard the *M.V. Northern Horizon* on June 9-20, 1999, at approximately 500 meters depth in the Eastern Mediterranean off the coast of Israel. The authors and collaborators employed JASON, with the navigation system described herein, to perform precise acoustic-bathymetric and photographic image surveys of ancient shipwrecks dating from approximately 750 B.C.

Figure 2 compares JASON vehicle navigation fixes obtained simultaneously using the LBL/Doppler system and the 300 kHz LBL system. The data was obtained during survey operations during JASON dive #250, June 17,

INSTRUMENT	VARIABLE	INTERNAL?	UPDATE RATE	PRECISION	RANGE	DRIFT
Acoustic Altimeter	Z - Altitude	yes	varies: 0.1-10Hz	0.01-1.0 m	varies	—
Pressure Sensor	Z - Depth	yes	medium: 1Hz	0.0.01%	full-ocean	—
Inclinometer	Roll and Pitch	yes	fast: 1-10Hz	0.1° - 1°	+/ − 45°	—
Magnetic Compass	Heading	yes	medium: 1-2Hz	$1 - 10°$	360°	—
Gyro Compass	Heading	yes	fast: 1-10Hz	0.1°	360°	$10°/hour$
12 kHz LBL	XYZ - Position	NO	varies: 0.1-1.0 Hz	0.01-10 m	5-10 Km	—
300 kHz LBL *	XYZ - Position	NO	1.0-5.0 Hz	+/-0.002 m typ	100 m	—
Ring-Laser Gyro *	Heading	yes	fast: 1-1600Hz	0.0018°	360°	$0.44°/hour$
Bottom-Lock Doppler *	XYZ - Velocity	yes	fast:1-5Hz	+/-0.2% - +/-1.0%	30m - 200m	—

Table 1: Underwater Vehicle Navigation Sensors. (*) indicates advanced sensors not yet in widespread use.

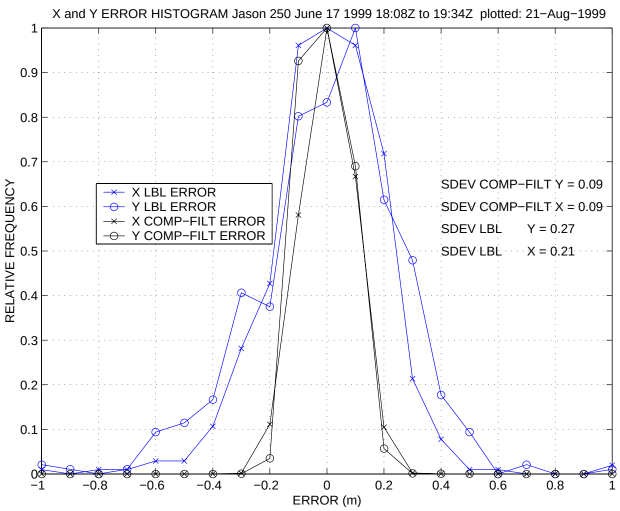

Figure 3: LBL/doppler vs LBL Navigation Precision: Histogram plots of of X and Y tracking errors. JASON dive #250 June 17 1999 18:08Z to 19:34Z.

1999, from 18:08Z to 19:34Z. Figure 3 shows histograms of the X and Y navigation errors observed during this vehicle deployment using (a) 12 kHz LBL navigation alone and (b) combined LBL/doppler navigation. The data show the 12 kHz LBL X and Y fixes to have zero mean and a standard deviation of 0.27 meter and 0.21 meter, respectively. The combined LBL/doppler system exhibits X and Y navigation errors with a standard deviation of 0.09 meter. Thus the LBL/doppler system is a factor of three more accurate than the LBL system alone. The LBL/doppler system provides vehicle position fixes every 0.25 second, while the the LBL system provides vehicle position fixes every 6.0 seconds — more than an order of magnitude improvement.

3 Acoustic and Optical Survey

Acoustic Survey

Narrow-beam sonars are the most widely used instruments for 3-D bathymetric surveys. Narrow-beam scanning sonars typically either have a single narrow beam that is mechanically "pointed" or have multiple beams in a fixed transducer head. Beam widths are typically $1° - 3°$. Ping frequencies range from 12 kHz (full-ocean depth range with accuracies of 10-100 meters) to 675 kHz (100 meter range with accuracies of 1-10cm. Sonar update rates are limited by the speed of sound in water, 1500 meters/second. The effective range resolution and area resolution of a single ping on the seafloor is limited by ping frequency and width. Sidescan sonars are used widely for 2-D searches and surveys, but relatively few sidescan systems are instrumented with the phase-sensitive transducers necessary for true 3-D bathymetry.

A typical UUV acoustic bathymetric survey proceeds as follows: the vehicle is navigated (using a precision navigation system) in a controlled grid-pattern above the seafloor site of interest, while a narrow-beam sonar simultaneously scans the bottom (See Figure 1). The world-referenced position of each individual sonar ping is computed from the ping's vehicle-referenced range, azimuth, and altitude, together with the vehicle's 6-DOF position and attitude. The precision of each ping's world coordinates depends on a surprising number of factors including sonar calibration, beam shape, vehicle sensor placement accuracy, and vehicle navigation accuracy. The world coordinates from an entire survey (typically numbering 10^4 to 10^6 pings) are then used to compute a bathymetric surface [28, 15]. Figure 5 (bottom) for example, shows the bathymetric map of a 4th Century B.C.E. Roman shipwreck at 800m depth obtained and computed the authors in the Mediterranean in June 1997. This geometrically precise three-dimensional representation of the wreck site was obtained with Jason ROV and a 675 kHz narrow-beam scanning sonar. This survey methodology, originally developed on the Jason ROV, has been adapted and deployed on the ABE autonomous underwater robot [37]. With recent improvements in sonar accuracy, navigation precision (Section 2) and the calibration of vehicle sensor placement have become the principal error sources in high resolution acoustic mapping.

Precise cross-calibration of the physical position and orientation of a vehicle's sonar and navigation sensors is critical. The problem is complicated by several factors: (*i*) pre-deployment calibration of attitude sensors is difficult or impossible aboard ship due to the ship's magnetic influence and the ship's natural motion; (*ii*) underwater sonars and cameras must be submerged for calibration; (*iii*) it often is impractical to repeatedly deploy purpose-built "sensor calibration targets"; (*iv*) working UUVs are often physically reconfigured for each dive — necessitating recalibration for each dive; (*v*) due to pressure and buoyancy effects, a deeply-submerged vehicle geometric dimensions differ significantly from those obtained in air — necessitating at-depth calibration. To address this problem, we are pursuing methods for precision *in-situ* sensor cross-calibration using naturally occurring benthic features. In [21] we report a novel technique for calibrating sonar attitude errors (roll, pitch, and yaw) as a nonlinear optimization problem. Additional problems involved in building high resolution bathymetric maps using narrow-beam sonars are addressed in [15]. To the best of our knowledge, the in-situ sensor calibration problem has not been previously addressed in the present context.

Optical Survey

Optical imaging using video, electronic still, and film cameras is employed extensively in oceanographic and forensic undersea operations. The technical obstacles to underwater optical imaging differ significantly from those found in land, air, and space imaging. Most of the technical obstacles in underwater optical imaging arise from the rapid attenuation and backscatter of light in the ocean.

First, underwater imagery is characterized by extremely uneven illumination. Backscatter and absorption affect underwater light severely, causing "hot spots" and poorly illuminated areas. This problem is exacerbated by the fact that an underwater vehicle must carry (and provide power for) both cameras and light sources. Since the light source moves with the sensor, shadows and "hot spots" move as well. High dynamic range camera systems, and the use of adaptive image processing techniques [22, 27] are both used to combat these problems but often they do so at the cost of obfuscating lighting cues that human operators rely on for depth perception.

Second, the ratio of target range to height disparity in the subject field is quite small. Underwater vehicle operators must frequently maneuver their vehicles through complex terrain whose relief is far greater than the vehicle's "flying" height. Under these conditions, parallax induced motion of terrain features in imagery can cause radically different views of objects to appear in successive images. The positions of objects in images is driven by the shape of the object as much as by the movement of the camera.

Third, the maximum single-image "footprint" is strictly limited by available illumination power, absorbtion, backscatter, and camera dynamic range. Objects larger than several meters cannot be captured with a single image — necessitating the use of photomosaicing techniques [9, 28, 10] to assemble a composite image from smaller individual images. At present, photomosaics are constructed by manually picking tie points between images and warping them using a variety of reprojections [12, 29, 3]. This process is illustrated in Figure 4. The completed mosaic, constructed by the authors, is comprised of 200 individual images. The mosaicing process introduces significant non-uniform geometric distortion in the resulting composite image — an effect that increases with the size of the mosiac [9, 28].

Techniques to automatically construct mosaics of underwater imagery, [16, 36], and to automate image image registration tasks, [20, 24], are the subject of active research. At present, these techniques are successful principally under ideal conditions including flat bottom, large field-of-view, uniform illumination, and constant vehicle altitude/attitude. These efforts are complicated by the fundamental limitations imposed by differential and moving lighting, and the movement of biota and particulate matter in the mosaic area, height disparity, and the fact that naturally occurring objects of interest are often unstructured [25].

We argue that successful solutions to the problem of automatically constructing geometrically accurate photomosaics ("quantitative photomosaics") will exploit the complementary nature of the acoustic and optical imaging data [10, 25]. Figure 5 illustrates the complementary nature of acoustic and optical imaging. The bathymetric map is a geometrically precise, yet lacks the level of detail present in the (intrinsically distorted) photomosaic. Our current work is focused on quantifying and removing geometric distortions through the use of complete three dimensional image reconstruction in photomosaics and on the implicit fusion of acoustic maps and photomosaics.

4 Conclusion

The theoretical and practical obstacles to underwater robotic survey missions differ from those in land, air, and space missions in several fundamental respects. The research obstacles and advances reported in Sections 2 and 3 will be only briefly amplified here.

Precision underwater vehicle navigation remains the principal obstacle to improved vehicle control. Newly available multi-beam doppler sonars can significantly augment existing 3-D underwater navigation systems. Experimental results with a new Doppler/LBL system show the system to outperform unaided doppler or LBL navigation alone. Precise navigation and control, however, is just one of several obstacles to precise, quantitative, and repeatable underwater survey operations. Precision surveys require fusion of data from variety of imaging sensors with differing ranges, resolutions, and physical principles. The fusion of precision acoustic bathymetric maps with optical imagery may enable the construction of geometrically precise photomosaics.

Acknowledgements

We gratefully acknowledge the invaluable support of the Deep Submergence Laboratory and the Deep Submergence Operations Group of the Woods Hole Oceanographic Institution.

References

[1] P. E. An, A. J. Healey, J. Park, and S. M. Smith. Asynchronous data fusion for AUV navigation via heuristic fuzzy filtering techniques. In *Proceedings of IEEE Oceans'97*, pages 397–402, October 1997.

[2] R. Bachmayer, S. Humphris, D. Fornari, C. V. Dover, J. Howland, A. Bowen, R. Elder, T.Crook, D. Gleason, W. Sellers, and S. Lerner. Oceanographic research using remotely operated underwater robotic vehicles: Exploration of hydrothermal vent sites on the mid-atlantic ridge at 37 north 32 west. *Marine Technology Society Journal*, 32(3):37–47, Fall 1998.

[3] R. D. Ballard. High tech search for roman shipwrecks. *National Geographic*, 193(4):32–42, April 1998.

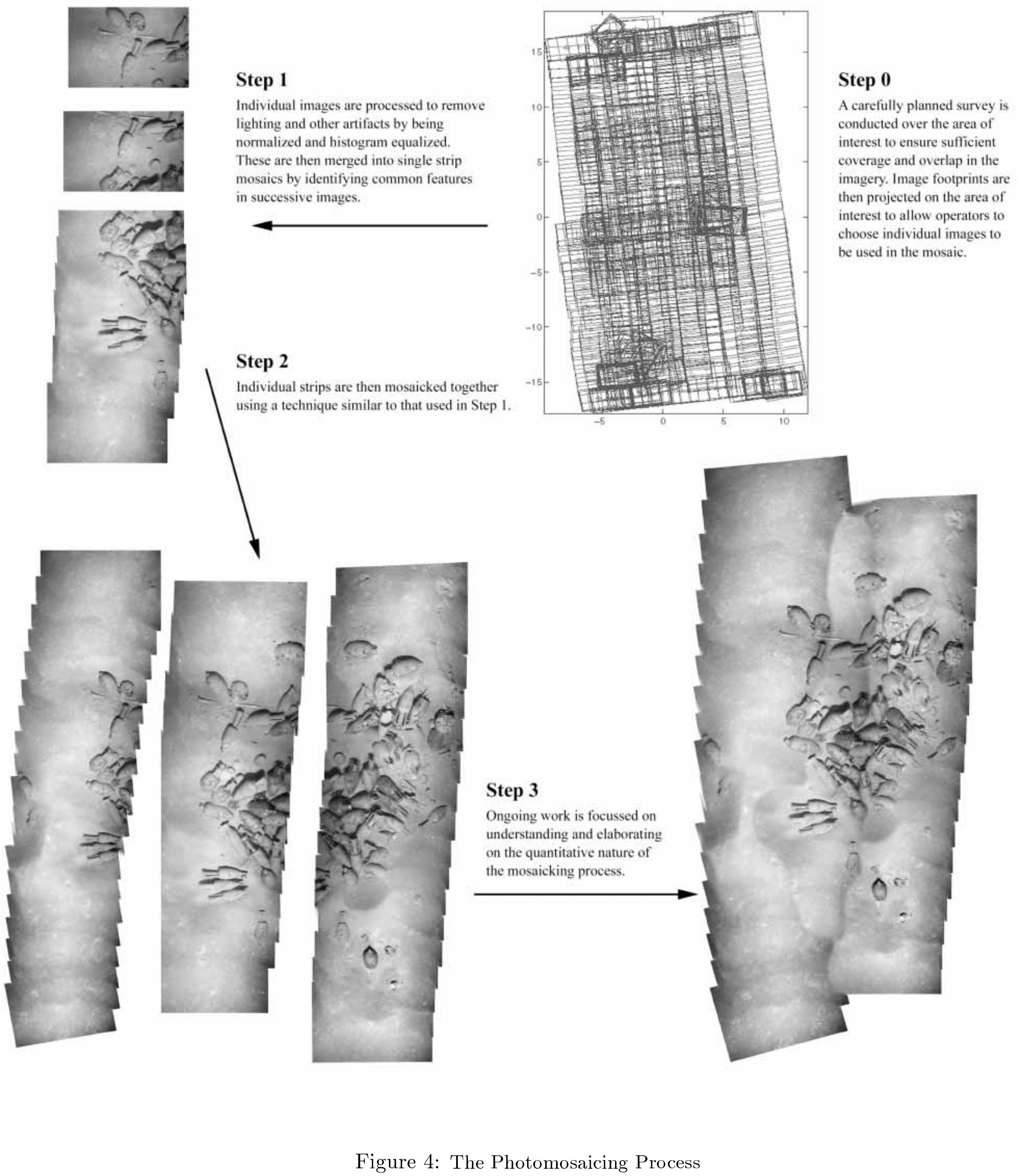

Figure 4: The Photomosaicing Process

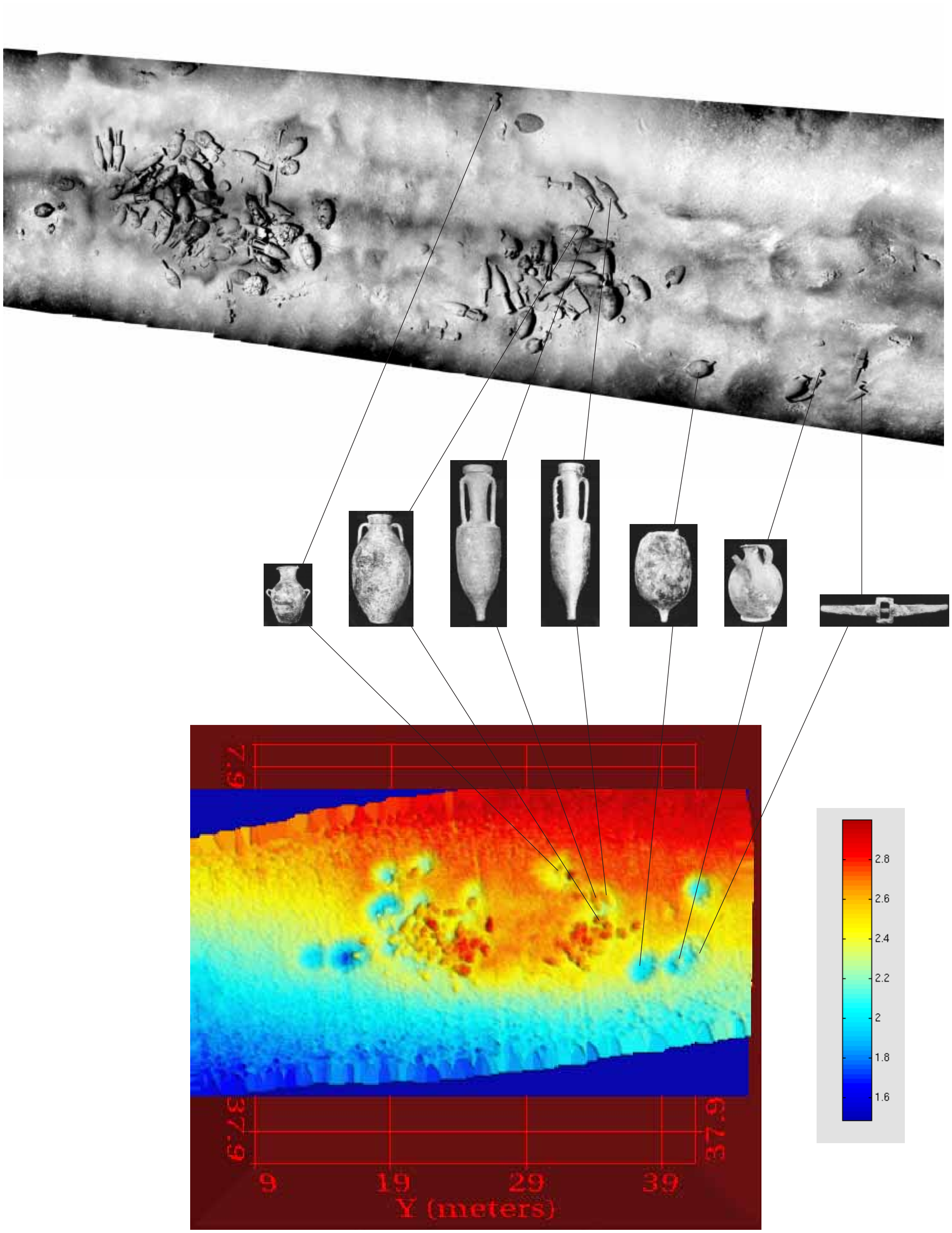

Figure 5: Optical Photomosaic (top) and Quantitative Acoustic Bathymetric Map (bottom). This 4th Century B.C.E. Roman shipwreck was surveyed with the Jason ROV at 800m depth by the authors in June 1997, at approximately 38°N 11°E in the Tyrrhenian Sea.

[4] B. M. Bell, B. M. Howe, J. A. Mercer, and R. C. Spindel. Nonlinear kalman filtering of long-baseline, short-baseline, gps, and depth measurements. In *Conference Record of the Twenty-Fifth Asilomar Conference on Signals, Systems and Computers*, pages 131–136, Pacific Grove, CA, USA, November 1991.

[5] N. Brokloff. Matrix algorithm for doppler sonar navigation. In *Proceedings of IEEE/MTS OCEANS'94*, volume 2, pages 378–83, September 1994.

[6] N. Brokloff. Dead reckoning with an ADCP and current extrapolation. In *Proceedings of IEEE/MTS OCEANS'97*, volume 2, pages 994–1000, October 1997.

[7] D. E. Dimassa and W. K. Stewart. Terrain-relative navigation for autonomous underwater vehicles. In *Proceedings of IEEE Oceans'97*, pages 541–546, Halifax, 1997.

[8] H. Feder, J. J. Leonard, and C. M. Smith. Adaptive sensing for terrain aided navigation. In *Proceedings of IEEE Oceans'98*, pages 336–341, Nice, 1998.

[9] J. B. Hersey. *Deep Sea Photography*. Johns Hopkins University Press, Baltimore, 1967.

[10] J. Howland, H. Singh, M. Marra, and D. Potter. Digital photomosaicking of underwater imagery. *Sea Technology*, pages 65–69, June 1999.

[11] M. M. Hunt, W. M. Marquet, D. A. Moller, K. R. Peal, W. K. Smith, and R. C. Spindell. An acoustic navigation system. Technical Report WHOI-74-6, Woods Hole Oceanographic Institution, Woods Hole, Massachusetts 02543 USA, December 1974.

[12] M. Kleinrock, S. Humphris, and the Deep-TAG Team. Detailed structure and morphology of the tag active hydrothermal mound and its geotectonic environment. In *Proceedings of the Ocean Drilling Program, Initial reports*, volume 158, pages 15–21. The Ocean Drilling Program, College Station, Texas, 1994.

[13] K. Kobayashi. Principal characteristics of the up-to-date japanese oceanographic research vessels. In *Proceedings of IEEE/MTS Oceans'95*, volume 1, pages 472–477, San Diego, 1995.

[14] M. Kyo, E. Hiyazaki, S. Tsukioka, H. Ochi, Y. Amitani, T. Tsuchiya, T. Aoki, and S. Takegawa. The sea trial of "kaiko", the full ocean depth research ROV. In *Proceedings. OCEANS '95 MTS/IEEE*, 1995.

[15] A. G. Lerner and L. L. Whitcomb. Acoustic micro-bathymetry data processing and rendering software: Release notes for version 2. Technical report, Dynamical Systems and Control Laboratory, Department of Mechanical Engineering, Johns Hopkins University, Baltimore, MD, September 1997.

[16] R. Marks, S. Rock, and M. Lee. Real-time video mosaicking of the ocean floor. *IEEE Journal of Oceanic Engineering*, 20(3):229–241, July 1995.

[17] P. H. Milne. *Underwater Acoustic Positioning Systems*. Gulf Publishing Company, Houston, 1983.

[18] J. Moryl, H. Rice, and S. Shinners. The universal gravity module for enhanced submarine navigation. In *Proc. IEEE 1998 Position Location and Navigation Symposium*, pages 324–331, Palm Springs, 1998.

[19] P. Newmand and H. Durrant-Whyte. Using sonar in terrain-aided underwater navigation. In *Proc. IEEE Int. Conf. Robt. Aut.*, pages 440–445, Leuven, 1998.

[20] S. Peleg and J. Herman. Panoramic mosaics by manifold projection. In *Proceedings of the 1997 IEEE Conference on Computer Vision and Pattern Recognition*, pages 338–343, San Juan, 1997.

[21] O. Pizarro, H. Singh, L. L. Whitcomb, and D. R. Yoerger. Towards in-situ sonar calibration for high-resolution bathymetric mapping with underwater robotic vehicles. In *Proc. IEEE Int. Conf. Robt. Aut.*, May 2000. (Under Review).

[22] S. M. Pizer, E. P. Amburn, J. D. Austin, R. Cromartie, A. Geselowitz, T. Greer, B. ter Haar Romeny, J. B. Zimmerman, and K. Zuiderveld. Adaptive histogram equalization and its variations. *Computer Vision, Graphics, and Image Processing*, 39(3):355–68, September 1987.

[23] RD Instruments Inc. ADCP coordinate transformations. Technical Report P/N 951-6079-00, RD Instruments Inc, 9855 Businesspark Avenue, San Diego, California, 92131, April 1997.

[24] H. S. Sawhney, S. Ayer, and M. Gorkani. Model based 2D and 3D dominant motion estimation for mosaicking and video representation. In *Proceedings of the IEEE Internatinal Conference on Computer Vision.*, pages 583–590, Cambridge, MA, 1995.

[25] H. Singh, J. Howland, D. Yoerger, and L. L. Whitcomb. Quantitative photomosaicing of underwater imaging. In *Proceedings of IEEE Oceans'98*, volume 1, pages 263–266, September 1998.

[26] R. C. Spindel, R. P. Porer, W. M. Marquet, and J. L. Durham. A high-resolution pulse-doppler underwater acoustic navigation system. *IEEE Journal of Oceanic Engineering*, 1(1):6–13, September 1976.

[27] J. A. Stark and W. J. Fitzgerald. An alternative algorithm for adaptive histogram equalization. *Graphical Models and Image Processing*, 58(2):180–85, March 1996.

[28] W. K. Stewart. High resolution optical and acoustic remote sensing for underwater exploration. *Oceanus*, 34(1):10–22, Spring 1991.

[29] M. M. Sulanowska, S. E. Humphris, and J. C. Howland. Detailed analysis of the surface morphology of the active TAG hydrothermal mound by mosaicking of digital images. *Transactions of the American Geophysical Union*, 77:768, 1996.

[30] J. Vaganay, J. G. Bellingham, and J. J. Leonard. Comparison of fix computation and filtering for autonomous acoustic navigation. *International Journal of Systems Science*, 29(10):1111–22, October 1998.

[31] S. Vajda and A. Zorn. Survey of existing and emerging technologies for strategic submarine navigation. In *Proc. IEEE 1998 Position Location and Navigation Symposium*, pages 309–315, Palm Springs, 1998.

[32] L. L. Whitcomb, D. R. Yoerger, and H. Singh. Advances in doppler-based navigation of underwater robotic vehicles. In *Proceedings of the IEEE International Conference on Robotics and Automation*, May 1999. (Invited paper).

[33] L. L. Whitcomb, D. R. Yoerger, H. Singh, and J. Howland. Combined doppler/LBL based navigation of underwater vehicles. In *Proceedings of the the 11th International Symposium on Unmanned Untethered Submersible Technology*, Durham, New-Hampshire, USA, August 1999.

[34] L. L. Whitcomb, D. R. Yoerger, H. Singh, and D. A. Mindell. Towards precision robotic maneuvering, survey, and manipulation in unstructured undersea environments. In Y. Shirai and S. Hirose, editors, *Robotics Research - The Eighth International Symposium*, chapter 2, pages 45–54. Springer-Verlag, London, 1998.

[35] R. A. Williams and R. Torchio. *M.V. Derbyshire Surveys — UK/EC Assessors Report: A Summary*. Department of the Environment, Transport and the Regions, Eland House,Bressenden Place, London SW1E 5DU, London, 1998. ISBN 1-85112-075-0.

[36] X. Xu and S. Negahdaripour. Vision-based motion sensing for underwater navigation and mosaicing of ocean floor images. In *Proceesdings of IEEE/MTS OOCEANS'97*, pages 1412–1417, 1997.

[37] D. R. Yoerger, A. M. Bradley, B. B. Walden, M.-H. Cromier, and W. Ryan. Fine-scale seafloor survey in rugged deep-ocean terrain with an autonomous robot. In *Proc. IEEE Int. Conf. Robt. Aut.*, May 2000. (Under Review).

[38] D. R. Yoerger, A. M. Bradley, B. B. Walden, H. Singh, and R. Bachmayer. Surveying a subsea lava flow using the autonomous benthic explorer (ABE). *International Journal of Systems Science*, 29(4):1031–1044, October 1998.

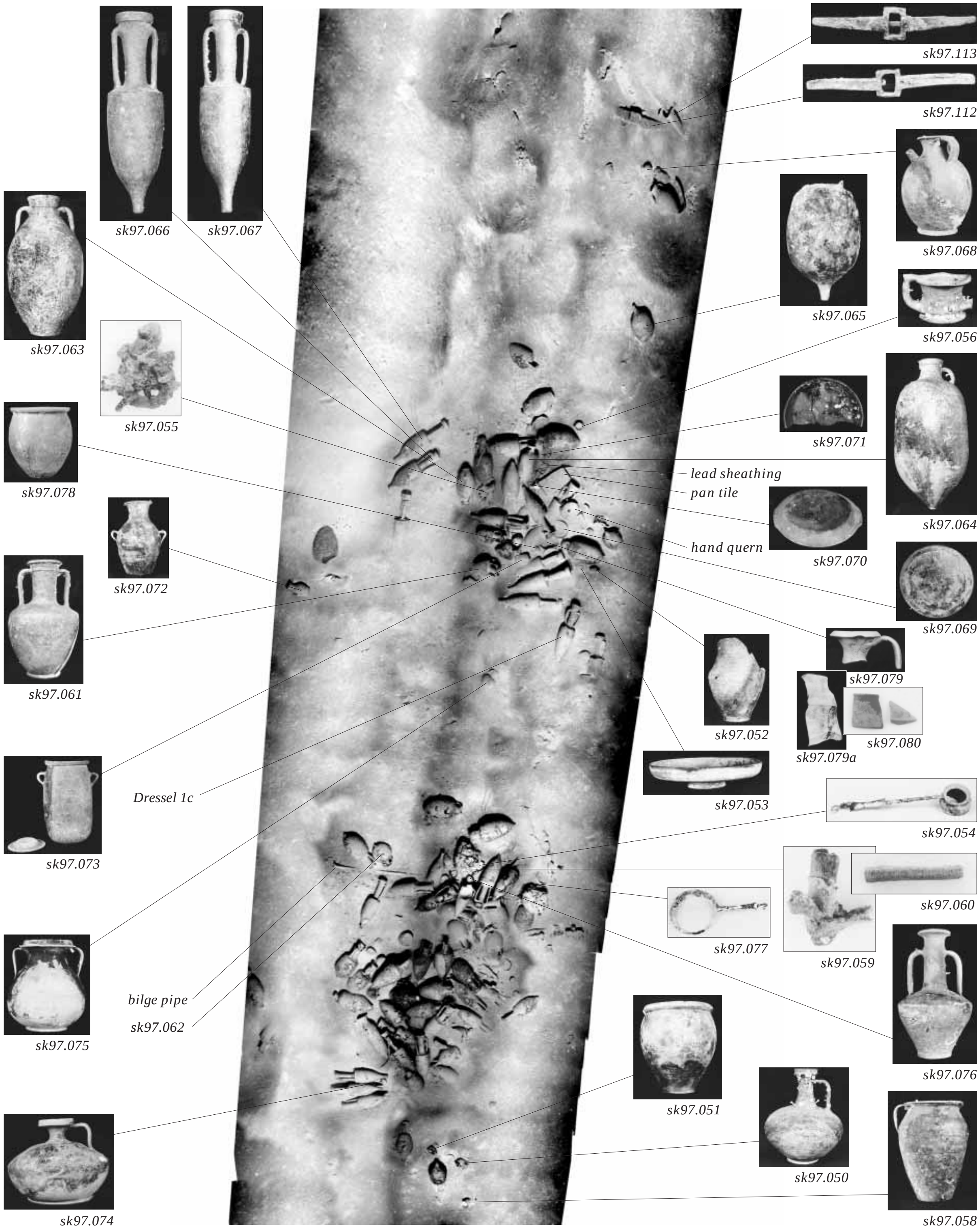

Figure 6: Photomosaic of 4th Century B.C.E. Roman shipwreck showing artifacts recovered for Archaeological study.